Vacuum 152 (2018) 8–14

Contents lists available at ScienceDirect

Vacuum

journal homepage: www.elsevier.com/locate/vacuum

Non-isothermal crystallization kinetics of $Fe_{75}Cr_5P_9B_4C_7$ metallic glass with a combination of desired merits

Tao Xu [a], Zengyun Jian [a, *], Fange Chang [a], Longchao Zhuo [b], Tao Zhang [c]

[a] School of Materials and Chemical Engineering, Xi'an Technological University, Xi'an 710021, Shaanxi, PR China
[b] School of Materials Science and Engineering, Xi'an University of Technology, Xi'an 710048, Shaanxi, PR China
[c] Key Laboratory of Aerospace Materials and Performance (Ministry of Education), School of Materials Science and Engineering, Beihang University, Beijing 100191, PR China

ARTICLE INFO

Article history:
Received 24 January 2018
Received in revised form
12 February 2018
Accepted 2 March 2018
Available online 3 March 2018

Keywords:
Fe-based metallic glass
Non-isothermal
Crystallization kinetics
Avrami exponent
Activation energy

ABSTRACT

The non-isothermal crystallization kinetics of our previously reported $Fe_{75}Cr_5P_9B_4C_7$ metallic glass (MG) was systematically evaluated by X-ray diffraction (XRD), transmission electron microscopy (TEM) and differential scanning calorimeter (DSC). The primary crystalline phases of the present alloy annealed under non-isothermal heating conditions were mainly identified as nanocrystalline α-(Fe,Cr), $(Fe,Cr)_3P$, $(Fe,Cr)_3C$ and $(Fe,Cr)_{23}(C,B)_6$ embedded in amorphous matrix by XRD and TEM. The apparent activation energy (E) for characteristic temperatures determined by Kissinger method is similar to that determined by Ozawa method. The E_g for the glass transition temperature is larger than both of the E_x for the onset crystallization temperature and the E_p for the peak temperature, indicating that the energy barrier for the glass transition is higher than that for the crystallization. Furthermore, the local activation energy evaluated by Kissinger-Akahira-Sunose (KAS) method and Ozawa-Flynn-Wall (OFW) method shows similar trend of gradual increase with the progressing of the crystallization process, implying that the improved difficulty of crystallization. Additionally, the local Avrami exponents gradually decreased from the values larger than 2.5 to the values smaller than 2.5, which implies a typical diffusion-controlled growth with variable crystallization mechanisms during the whole process.

1. Introduction

Fe-based metallic glasses (MGs) possess marvelous advantages for using as the potential engineering and functional materials due to their excellent soft-magnetic properties, i.e., high saturation magnetization, high permeability, low coercivity and low core loss, high corrosion and wear resistance, high fracture strength and high hardness, which have attracted great attentions of scientific and industrial researchers [1–15]. Accordingly, a great deal of efforts should be devoted to the synthesis of novel Fe-based MGs and the exploration of their formation and properties.

Previous researches have revealed that the study on crystallization kinetics under non-isothermal conditions plays a key role for understanding the formation and properties of MGs [16–33]. On one hand, it can provide helpful information on the nucleation and growth processes of crystalline phases [31,32], which is of great importance for tunable properties of MGs such as soft-magnetic properties. On the other hand, quantitative analysis relevant to the thermal stability and mechanisms for crystallization of MGs can be deduced by calculating the thermodynamic and kinetic data such as the activation energy of crystallization and Avrami exponent [33], which is beneficial for producing new MGs with desirable glass-forming ability (GFA).

Recently, we developed a novel $Fe_{75}Cr_5P_9B_4C_7$ MG with combined advantages of high GFA, good magnetic properties, excellent corrosion resistance, high fracture strength, high Vickers microhardness and cost-effectiveness only using industrial ferro-alloys without high-purity materials, which exhibits an analogous GFA and comparable properties to the MG with similar composition prepared using high-purity materials, showing great potential for industrial applications [34]. Consequently, it is of great importance to evaluate the crystallization kinetics for the newly developed $Fe_{75}Cr_5P_9B_4C_7$ MG. In this work, the crystallization kinetics of $Fe_{75}Cr_5P_9B_4C_7$ MG under non-isothermal heating conditions was systematically investigated using differential scanning calorimeter (DSC) and analyzed by various approaches of Kissinger, Ozawa,

* Corresponding author.
E-mail address: zengyunjian@xatu.edu.cn (Z. Jian).

https://doi.org/10.1016/j.vacuum.2018.03.003
0042-207X/

Johnson-Mehl-Avrami, Kissinger-Akahira-Sunose and Ozawa-Flynn-Wall. Besides, the crystallization mechanism was discussed.

2. Experimental procedure

Ingots with the nominal composition of $Fe_{75}Cr_5P_9B_4C_7$ were prepared by induction melting mixtures of industrial ferro-alloys in an argon atmosphere. Ribbons with a dimension of 2 mm in width and ~20 μm in thickness were produced by single-roller melt spinning. It is noted that the chamber for preparation of the ingots and ribbons of the present alloy was firstly pumped to the pressure lower than 1.0×10^{-2} Pa and then inlet argon gas, preventing the ingots and ribbons from deterioration by oxygen and other harmful atmosphere. The fabrication of the present $Fe_{75}Cr_5P_9B_4C_7$ alloy is previously described in details in Ref. [34]. The structure of as-cast and annealed specimens was examined by X-ray diffraction (XRD) using a SHIMADU XRD-6000 X-ray diffractometer with Cu-$K\alpha$ radiation and JEM-2010 transmission electron microscopy (TEM). The non-isothermal crystallization kinetics of the glassy ribbons was characterized by continuous heating with various heating rates (10–50 K min^{-1}) until full crystallization using a METTLER-TOLEDO TGA/DSC1 differential scanning calorimeter under flowing purified argon atmosphere within the error of ±2 K. The annealed specimens for XRD and TEM measurements of the present alloy were obtained by continuous heating from ambient temperature to the first peak temperature under various rates (10–50 K min^{-1}) then with furnace cooling in the METTLER-TOLEDO TGA/DSC1 sample chamber in flowing purified argon atmosphere.

3. Results and discussion

Fig. 1 exhibits the XRD pattern of as-cast $Fe_{75}Cr_5P_9B_4C_7$ alloy. It is shown that there is only a broad diffuse halo without any appreciable crystalline phase for the as-cast alloy, demonstrating a typical amorphous structure.

Fig. 2 shows the DSC curves (solid lines) of the $Fe_{75}Cr_5P_9B_4C_7$ MG at the continuous heating with rates of 10 K min^{-1}, 20 K min^{-1}, 30 K min^{-1}, 40 K min^{-1} and 50 K min^{-1}, respectively. It can be seen that all of the DSC curves depict an obvious glass transition with a supercooled liquid region, followed by distinct exothermic peaks corresponding to the crystallization of the $Fe_{75}Cr_5P_9B_4C_7$ MG, which further confirms the amorphous nature of the alloy. Meanwhile, it exhibits that the characteristic temperatures, i.e., the glass

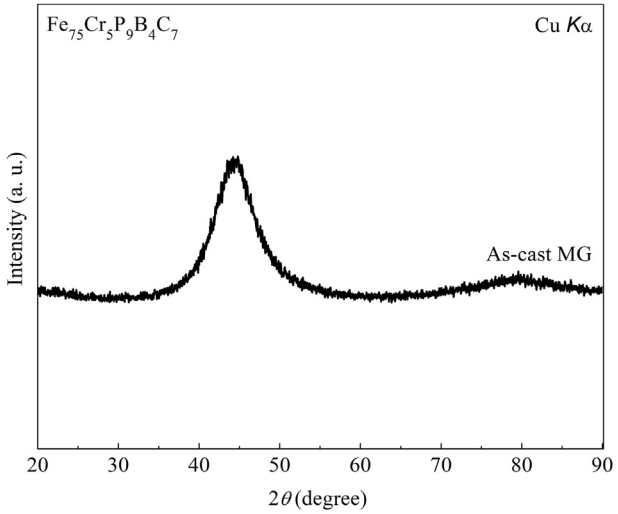

Fig. 1. XRD pattern of as-cast $Fe_{75}Cr_5P_9B_4C_7$ alloy.

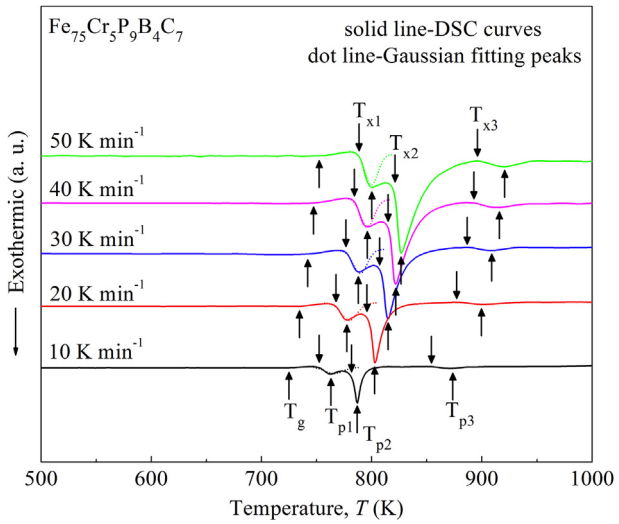

Fig. 2. DSC curves (solid lines) of the $Fe_{75}Cr_5P_9B_4C_7$ MG at continuous heating with respective rates of 10 K min^{-1}, 20 K min^{-1}, 30 K min^{-1}, 40 K min^{-1} and 50 K min^{-1}. Note: dot lines are Gaussian fitting peaks for the first crystallization peaks.

transition temperature (T_g), the first onset crystallization temperature (T_{x1}), the first peak temperature (T_{p1}), the second onset crystallization temperature (T_{x2}), the second peak temperature (T_{p2}), the third onset crystallization temperature (E_{x3}) and the third peak temperature (E_{p3}), shift to higher temperatures with the increase of the heating rates, and the supercooled liquid region ($\Delta T_x = T_{x1} - T_g$) expands, indicating that both the glass transition and crystallization depend on the heating rates during continuous heating. The values of T_g, T_{x1}, T_{p1}, T_{x2}, T_{p2}, T_{x3}, T_{p3} and ΔT_x for the $Fe_{75}Cr_5P_9B_4C_7$ MG are summarized in Table 1.

It is suggested that the apparent activation energy (E) of characteristic temperatures under the non-isothermal heating conditions, i.e., E_g of the glass transition temperature, E_{x1} of the first onset crystallization temperature, E_{p1} of the first peak temperature, E_{x2} of the second onset crystallization temperature, E_{p2} of the second peak temperature, E_{x3} of the third onset crystallization temperature and E_{p3} of the third peak temperature, can be used to illustrate the crystallization process, which is widely determined by Kissinger method [35] and Ozawa method [36]. For the Kissinger method, it is given as [35]:

$$ln\left(\frac{T^2}{\varphi}\right) = \frac{E}{RT} + c_1 \quad (1)$$

where φ is the heating rate, R is the gas constant, c_1 is a constant, T represents the characteristic temperatures, such as T_g, T_{x1}, T_{p1}, T_{x2}, T_{p2}, T_{x3} and T_{p3}, E is the apparent activation energy of characteristic temperatures corresponding to E_g, E_{x1}, E_{p1}, E_{x2}, E_{p2}, E_{x3} and E_{p3}, respectively. E can be obtained from the slopes of the linear fitting plots of $\ln(T^2/\varphi)$ versus $1000/T$ using Eq. (1). Fig. 3(a) exhibits these plots of T_g, T_{x1}, T_{p1}, T_{x2}, T_{p2}, T_{x3} and T_{p3}. As can be seen, the plots are approximately straight lines. Hence, E_g, E_{x1}, E_{p1}, E_{x2}, E_{p2}, E_{x3} and E_{p3} can be determined, and the results are listed in Table 2.

Meanwhile, the E determined by Ozawa method can be expressed as [36]:

$$ln(\varphi) = -1.0516\frac{E}{RT} + c_2 \quad (2)$$

where c_2 is a constant. E can be calculated from the slopes of the linear fitting plots of $\ln(\varphi)$ versus $1000/T$ by Eq. (2). Fig. 3(b) shows a